

Partially Overlapping Tones for Uncoordinated Networks

Alphan Şahin¹, Erdem Bala², İsmail Güvenc³, Rui Yang², and Hüseyin Arslan¹

¹Department of Electrical Engineering, University of South Florida, Tampa, FL, 33620

²InterDigital Communications Inc., Huntington Quadrangle, Melville, NY 11747

³Department of Electrical and Computer Engineering, Florida International University, Miami, FL, 33174

Email: alphan@mail.usf.edu, erdem.bala@interdigital.com, iguvenc@fiu.edu,
rui.yang@interdigital.com, arslan@usf.edu

Abstract—In an uncoordinated network, the link performance between the devices might degrade significantly due to the interference from other links in the network sharing the same spectrum. As a solution, in this study, the concept of *partially overlapping tones (POT)* is introduced. The interference energy observed at the victim receiver is mitigated by partially overlapping the individual subcarriers via an intentional carrier frequency offset between the links. Also, it is shown that while orthogonal transformations at the receiver cannot mitigate the other-user interference without losing spectral efficiency, non-orthogonal transformations are able to mitigate the other-user interference without any spectral efficiency loss at the expense of self-interference. Using spatial Poisson point process, a tractable bit error rate analysis is provided to demonstrate potential benefits emerging from POT.

Index Terms—non-orthogonal schemes, partially overlapping tones, Poisson point process, uncoordinated networks, waveform.

I. INTRODUCTION

Traditional broadband wireless networks have been strained with emerging demands such as being always-connected to the network and very high throughput to satisfy data-hungry applications such as real-time video. Satisfaction of these demands constitutes the main driving force for heterogeneous networks (HetNets) in which multiple tiers with varying coverage co-exist over the same network. In HetNets, interference among the tiers or the devices might dominate the noise and create interference-limited networks. The interference issues become prominent especially when dense and unplanned deployments such as device-to-device (D2D) communications are taken into account. Considering this issue, a new technique in which certain features of the waveform itself are used to mitigate the interference is proposed.

A waveform, which is one of the core elements determining the characteristics of a communication system, describes the formation of associated resources in signal space [1], [2]. Robustness of the transmitted signal to dispersion in the transmission medium, channel access, and hardware complexity are just few features affected by the selected waveform. Hence, waveform design should be able to address the requirements specified by the system. When the performance of the network is limited by noise, main consideration for the waveform design can naturally be on individual link properties such as reducing the interference created by the time and frequency dispersion of the channel [3]. However, interference created by other users is many times a major factor limiting the

performance of a network and as such the impact of the other-user interference might be more significant compared to the interference due to the channel dispersion. *Conventionally*, the interference between the devices are elaborated with the approaches which question the amount of the interference power at the receiver location without including the impact of the waveform itself. Most of the solutions devised to address the interference problem rely either on media access control (MAC) based coordination or interference cancellation. For example, interference coordination mechanisms with proper scheduling and resource allocation aim to minimize the interference power [4]. In physical layer, methods like interference cancellation [5], multiuser detection [6], and interference alignment [7] handle the other-user interference by exploiting the difference between desired and interfering signal strengths, codes, and multipath channel.

As opposed to the conventional solutions, in this paper, a new concept based on utilizing the time-frequency characteristics of waveforms to reduce the other-user interference is proposed. The main contributions of this paper are:

- We introduce the concept of partially overlapping tones (POT) in which it is allowed for subcarriers allocated to interfering links to partially overlap. The overlap is achieved by introducing an intentional CFO between the links and its amount is controlled by appropriately designing the time-frequency utilization of the waveforms.
- It is shown that with orthogonal waveforms, there is a tradeoff between other-user interference and spectral efficiency. Mitigation of the other-user interference can be achieved at the expense of a loss in spectral efficiency.
- It is further shown that with non-orthogonal waveforms, there is a tradeoff between other-user interference and self-interference. Mitigation of the other-user interference can be achieved at the expense of increased self-interference while spectral efficiency remains unchanged.
- A tractable bit error rate (BER) analysis for an uncoordinated network deployment is provided. The analysis allows to understand the system performance for various network densities and waveform designs.

The rest of paper is organized as follows: Related work is discussed in Section II. The system model including the physical layer parameters is provided in Section III while the concept of POT for orthogonal and non-orthogonal waveform structures is introduced in Section IV. Then, BER analysis

is provided in Section V and numerical results evaluating the performance of the proposed approach are provided in Section VI. Finally, the paper is concluded in Section VII.

II. RELATED WORK

The concept of overlapping wireless channels exists within the several 802.11 families (e.g. Wi-Fi systems). However, the simultaneous access to the channels is usually avoided due to interference. The utilization of overlapping channels to improve throughput has been investigated in several papers [8]–[13]. In [8], it is emphasized that the channel separation between the two pairs of Wi-Fi nodes can be interpreted as the physical separation between the nodes. Therefore, if partially overlapping channels are used carefully, it can provide greater spatial re-use. These papers consider the total spectrum utilization of the transmission, and do not show the impact of the partial overlapping on *individual subcarriers*. To the best of our knowledge, detailed time-frequency analysis on the interference due to the partially overlapping pulse shapes is not available in the literature.

Some of the challenging aspects of the other-user interference are its asynchronous nature and its statistical characterization, which depend on the deployment model and waveform structure utilized in the network. Orthogonal frequency division multiplexing (OFDM) is a well-investigated multicarrier scheme in case of asynchronous interference, e.g., femtocell-macrocell coexistence [14]–[16]. By providing some timing offset between the tiers intentionally, the different types of the interference, i.e. inter-carrier interference (ICI) and inter-symbol interference (ISI), is converted into each other in [16]. Yet, the total other-user interference is kept constant. A theoretical BER analysis investigating ISI versus ICI trade-offs in OFDM downlink is provided in [17]. In [18], BER degradation due to the adjacent channel interference is investigated by emphasizing superiority of filter bank multicarrier (FBMC) based cellular systems over an OFDM based approach. Although these investigations provide useful intuitions on the performance degradation, the analyses are performed for idealistic assumptions, such as grid-based cell deployment and uniform user density. In [19], it is emphasized that even if the geographical user density is uniform, the distance of the users linked to the corresponding serving points might not be uniform due to the irregular base station deployment and shadowing characteristics. In [20], [21], homogeneous Poisson point processes (PPPs) are considered to model the deployment of the base stations. This approach, which is pessimistic compared to highly idealized grid-based models and real deployment scenarios, yields a tractable tool which exploits the stochastic geometry. In the following studies, e.g., [22] and [23], analytical models for uplink and K -tier heterogeneous networks are provided using PPPs.

Investigation on the impact of PPPs on physical layer is limited, but available. For example, coexistence between ultra wide band (UWB) and narrow band systems is investigated using PPPs and impact of pulse shape is emphasized for aggregate network emission [20]. In [24], error rate analyses are provided for quadrature amplitude modulation (QAM) and

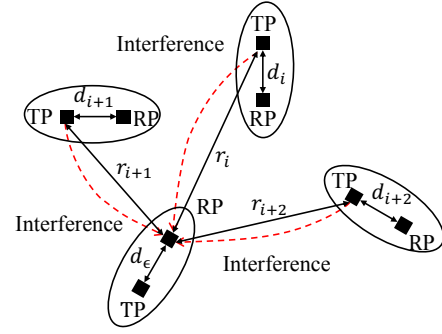


Fig. 1. Illustration of interference in an uncoordinated network.

phase shift keying (PSK) modulations using PPPs, excluding the impact of waveforms.

III. SYSTEM MODEL

Consider an uncoordinated network where transmission points (TPs) and their corresponding reception points (RPs) are distributed in an area as a realization of homogeneous 2-D PPP of Φ with the intensity λ as in Fig. 1. Interfering TPs and the RP investigated are called as *aggressors* and *victim*, respectively. Without any loss of generality, victim is located at the origin of the polar coordinates (0,0). The distance between the i th aggressor and the victim is given as r_i . Minimum distance between the aggressors and the victim is set to r_{\min} . While the distance between RP and its associated TP for i th aggressor link is denoted by d_i , the same distance is expressed by d_ϵ for the desired link for the victim. Also, it is assumed that aggressors are farther away than d_ϵ , i.e., $r_i > r_{\min} \geq d_\epsilon$, which is widely considered for the interference analyses based on PPPs [25].

In the following subsections, signal model for transmission and reception based on multicarrier schemes and channel model that includes large and small scale effects are given for further discussions on POT.

A. Signal Model for Transmission

The transmitted signal from the desired TP and the transmitted signals from the i th aggressor can be expressed as

$$s^\epsilon(t) = \sum_{n=-\infty}^{\infty} \sum_{l=0}^{N-1} X_{nl}^\epsilon g_{nl}^\epsilon(t), \quad (1)$$

and

$$s^i(t) = \sum_{n=-\infty}^{\infty} \sum_{l=0}^{N-1} X_{nl}^i g_{nl}^i(t), \quad (2)$$

respectively, where X_{nl}^ϵ and X_{nl}^i are the information symbols which are independent and identically distributed (i.i.d.) with zero mean on the l th subcarrier and n th symbol, N is the number of subcarriers, and $g_{nl}^\epsilon(t)$ and $g_{nl}^i(t)$ are the *synthesis functions* which map information symbols into time-frequency plane based on a rectangular lattice as

$$g_{nl}^\epsilon(t) = g^\epsilon(t - n\tau_0) e^{j2\pi l\nu_0 t} \quad (3)$$

and

$$g_{nl}^i(t) = g^i(t - n\tau_0) e^{j2\pi\nu_0 t} . \quad (4)$$

The family of functions in (3) and (4) are often referred to as *Gabor frame* or *Weyl-Heisenberg frame*, where $g^\epsilon(t)$ and $g^i(t)$ are the prototype filters employed at the transmitters, ν_0 is the subcarrier spacing and τ_0 is the symbol spacing [26], [27]. For the sake of notation simplicity, ν_0 and τ_0 are given in units of F and T , respectively (e.g., $\nu_0 = 1.2 \times F$ and $\tau_0 = 1.3 \times T$), where $F = 1/T$ and F is a number based on the design. Without loss of generality, the energy of $g^\epsilon(t)$ and the energy of $g^i(t)$ are normalized as

$$\|g^\epsilon(t)\|_{\mathcal{L}^2(\mathbb{R})}^2 = \|g^i(t)\|_{\mathcal{L}^2(\mathbb{R})}^2 = \int_{-\infty}^{\infty} |g^\epsilon(t)|^2 dt = 1 , \quad (5)$$

where $\mathcal{L}^2(\mathbb{R})$ denotes the square-integrable function space over \mathbb{R} and $\|\cdot\|$ is the \mathcal{L}^2 -norm of function.

B. Large Scale Impacts

Considering various path loss models depending on the environment, the path loss is characterized by $L_m(\cdot) = a + b \log_{10}(\cdot)$ where the path loss parameters a and b are scalars and the argument is the distance in meters. The received interference power from the i th aggressor and the desired signal power at victim location per subcarrier are denoted by P_i and P_ϵ , respectively. Impact of shadowing is not considered in this study. Main reason for this issue is to give insights on the POT rather than introducing extra complexity for the system model. However, using the methodologies proposed for the moment generation function of the summations of lognormal distributed lognormal variables [28] and [29], it is possible to include the impact of shadowing on the investigation.

For the link transmission, open loop fractional power control is applied and some amount of the path loss, i.e., $\beta(a + b \log_{10}(\cdot))$, is compensated, where $\beta \in [0, 1]$ is the path loss compensation parameter. Note that TP might transmit with the maximum transmit power in some cases. However, since link distances considered are small, the possibility of transmission at maximum power is excluded.

C. Small Scale Impacts

Time-varying multipath channel is taken into account between all RPs and TPs. Channel impulse response is characterized by $h(\tau, t) = \sum_{\ell=0}^{L-1} \varrho_\ell(t) \delta(\tau - \tau_\ell)$ where L denotes the total number of multipaths, ℓ is the path index, and τ_ℓ is the delay of the ℓ th path. It is assumed that the path gains, $\varrho_\ell(t)$, are independent and identically distributed variables and the signals experience Rayleigh fading, which is a common model for interference analysis. Also, the expected channel power is considered as $\sum_{\ell=0}^{L-1} \mathbb{E} [|\varrho_\ell(t)|^2] = 1$. For the sake of notation, the channel between i th interfering TP and the victim RP and the channel between desired TPs and the victim RP are expressed as $h_i(\tau, t)$ and $h_\epsilon(\tau, t)$, respectively.

D. Synchronization

As discussed in [30] and [31], synchronization to the received signal in the presence of interference might be challenging, especially at low signal-to-interference-plus-noise ratio (SINR)s. However, the impairments like timing offset and carrier frequency offset (CFO) are often related to the preamble structure rather than the data portion of the frame. Therefore, perfect synchronization at the pair of interest is assumed. Besides, timing misalignment between the aggressor's signals and synchronization point of the victim is taken into account. The timing misalignment of i th aggressor signal with respect to the synchronization point of the victim RP is denoted by Δt_i and its distribution $f_{\Delta t_i}(\Delta t_i)$ is assumed as uniform between 0 and τ_0 . Besides, intentional CFO between i th aggressor and the victim RP is given by Δf_i in order to generate POT which is discussed in Section IV. The impact of CFO due to the hardware mismatches between the aggressor's signals and desired signal is ignored. This is because of the fact that the impact of CFO due to the hardware mismatches is relatively smaller than Δf_i for POT. For example, when carrier spacing is set to 15 kHz and CFO is 500 Hz, normalized CFO becomes 0.033 (500 Hz / 15 kHz). However, the amount of normalized Δf_i for POT, throughout the study, is at least 0.5, which is significantly larger than CFO due to the hardware error.

E. Signal Model for Reception

Considering all interfering TPs, and assuming a wide-sense stationary uncorrelated scattering (WSSUS) channel model [32], the received signal at the victim is obtained as

$$\begin{aligned} r(t) = & \underbrace{\sqrt{P_\epsilon} \int_{\tau} \int_{\nu} H_\epsilon(\tau, \nu) s^\epsilon(t - \tau) e^{j2\pi\nu t} d\nu d\tau}_{\text{Desired signal}} \\ & + \underbrace{\sum_{i \in \Phi} \sqrt{P_i} \int_{\tau} \int_{\nu} H_i(\tau, \nu) s^i(t + \Delta t_i - \tau) e^{j2\pi\nu t} d\nu d\tau}_{\text{Interfering signals}} + \underbrace{w(t)}_{\text{Noise}} \end{aligned} \quad (6)$$

where $H_\epsilon(\tau, \nu)$ and $H_i(\tau, \nu)$ are the Fourier transformations of $h_\epsilon(\tau, t)$ and $h_i(\tau, t)$, respectively, and $w(t)$ is the additive white Gaussian noise (AWGN) with zero mean and variance σ_{noise}^2 . In order to get the information symbol on the k th subcarrier and m th symbol, the received signal is correlated by the *analysis function* where

$$\gamma_{mk}^\epsilon(t) = \gamma^\epsilon(t - m\tau_0) e^{j2\pi k\nu_0 t} . \quad (7)$$

Then, the output of the correlator is sampled with the sampling period to obtain the received symbol as

$$\begin{aligned} \tilde{X}_{mk}^\epsilon &= \langle r(t), \gamma_{mk}^\epsilon(t) \rangle \triangleq \int_t r(t) \gamma_{mk}^{\epsilon*}(t) dt \\ &= \underbrace{\sqrt{P_\epsilon} X_{mk}^\epsilon A_{mkmk}^\epsilon}_{\text{desired part}} + \underbrace{\sqrt{P_\epsilon} \sum_{\substack{n=-K+1 \\ n \neq m}}^{K-1} \sum_{\substack{l=0 \\ l \neq k}}^{N-1} X_{nl}^\epsilon A_{nlmk}^\epsilon}_{\text{self-interference part}} \\ &\quad + \underbrace{\sum_{i \in \Phi} \sqrt{P_i} \sum_{n=-K+1}^{K-1} \sum_{l=0}^{N-1} X_{nl}^i A_{nlmk}^i}_{\text{other-user interference}} + \underbrace{W_k}_{\text{noise}}. \end{aligned} \quad (8)$$

In (8),

$$A_{nlmk}^\epsilon = \int_\tau \int_\nu H_\epsilon(\tau, \nu) \int_t g_{nl}^\epsilon(t - \tau) \gamma_{mk}^{\epsilon*}(t) e^{j2\pi\nu t} dt d\nu d\tau, \quad (9)$$

$$\begin{aligned} A_{nlmk}^i &= \int_\tau \int_\nu H_i(\tau, \nu) \int_t g_{nl}^i(t - \Delta t_i - \tau) e^{j2\pi\Delta f_i(t - \Delta t_i - \tau)} \\ &\quad \times \gamma_{mk}^{\epsilon*}(t) e^{j2\pi\nu t} dt d\nu d\tau, \end{aligned} \quad (10)$$

and they show the correlation between the symbols (n, l) and (m, k) including the dispersion due the channel. As it is seen in (8), while other-user interference is caused by aggressor links, self-interference can occur due to the time-varying multipath channel, hardware impairments, or non-Nyquist filter utilization. Considering (8), SINR can be expressed as

SINR =

$$\frac{\underbrace{|A_{mkmk}^\epsilon|^2}_{G_\epsilon}}{\underbrace{\sum_{\substack{n=-K+1 \\ n \neq m}}^{K-1} \sum_{\substack{l=0 \\ l \neq k}}^{N-1} |A_{nlmk}^\epsilon|^2}_{I_{\text{self}}} + \underbrace{\sum_{i \in \Phi} \frac{P_i}{P_\epsilon} \sum_{n=-K+1}^{K-1} \sum_{l=0}^{N-1} |A_{nlmk}^i|^2}_{G_i} + \frac{\sigma_{\text{noise}}^2}{P_\epsilon}}_{I_i}} + \frac{\sigma_{\text{noise}}^2}{P_\epsilon} \quad (11)$$

where K is the filter length in terms of symbol spacing, I_{total} is the total interference, I_{self} and I_{other} are the self-interference and other-user interference, respectively, I_i is the interference due to i th aggressor, G_ϵ and G_i are the interference gains including fading and filter characteristics, and

$$\frac{P_i}{P_\epsilon} = d_\epsilon^{\frac{b-\beta b}{10}} d_i^{\frac{\beta b}{10}} r_i^{-\frac{b}{10}}. \quad (12)$$

Note that K is related to the representation of the filter in time domain. As long as K is selected properly, the filter truncation has a minor impact on self-interference compared to the interference due to the time-varying multi-path channel or hardware impairments at the RP and/or TP. While G_ϵ is a random variable with unit mean exponential distribution because of the Rayleigh fading [17], [18], G_i can be characterized for

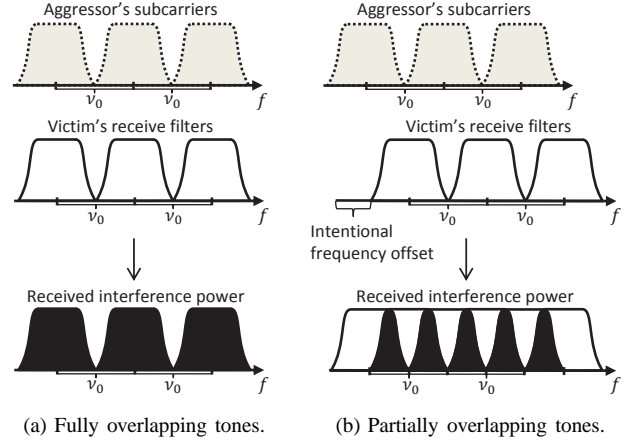


Fig. 2. Illustrations for full overlapping and partial overlapping. While full-overlapping tones cause significant other-user interference, the main portion of the interference is mitigated by the receive filter with the concept of POT.

a given Δt_i and Δf_i by exponential distribution where its mean is given by

$$\sigma_i^2(\Delta t_i, \Delta f_i) = \sum_{n=-K+1}^{K-1} \sum_{l=0}^{N-1} |g_{nl}^i(t - \Delta t_i) e^{j2\pi\Delta f_i t}, \gamma^\epsilon(t)|^2, \quad (13)$$

Conventionally, $\sigma_i^2(\Delta t_i, \Delta f_i)$ is considered as 1 for link-level analyses [21], similar to the mean of G_ϵ . However, expressing it as in (13) gives flexibility to include the impact of transmit and receive filters and calculate interference when an additional processing is performed to reduce other-user interference. Finally, I_{self} is also a random variable with exponential distribution where, considering the Rayleigh fading assumption [18], its mean is given by

$$\sigma_{\text{self}}^2 = \sum_{\substack{n=-K+1 \\ n \neq m}}^{K-1} \sum_{\substack{l=0 \\ l \neq k}}^{N-1} |g_{nl}^\epsilon(t), \gamma^\epsilon(t)|^2. \quad (14)$$

Essentially, calculations of both σ_{self}^2 and $\sigma_i^2(\Delta t_i, \Delta f_i)$ are based on the projection operation onto receive filters, which can be derived via corresponding ambiguity functions [2].

IV. PARTIALLY OVERLAPPING TONES

The main goal of the POT is to mitigate other-user interference given in (13) by using the waveform structure. It relies on intentional CFO between aggressor's Gabor system and victim's Gabor system. For example, while one of the links operates at carrier frequency f_c , the other link operates at $f_c + \nu_0/2$. By allowing this operation, instead of full-overlapping between the subcarriers of the links, POT is obtained. This approach also fits the asynchronous nature of other-user interference as it does not introduce any timing constraint between interfering signals. One can interpret the intentional CFO as an alignment strategy in frequency domain.

In Fig. 2, a motivating example based on filtered multitone (FMT) is illustrated for POT. In FMT, each subcarrier is generated via a band-limited filter [33]. As opposed to the

conventional understanding of OFDM, the subcarriers are not overlapped in frequency domain. By providing additional guard bands, orthogonality between subcarriers is maintained. Note that these guard bands are also useful to provide immunity against self-interference due to the time-frequency impairments. In the provided example in Fig. 2, these guard bands are exploited further and they are used to mitigate the other-user interference. By applying an intentional CFO between two different links, other-user interference mitigation is provided in an uncoordinated network.

POT is fundamentally related to the utilization of the time-frequency plane by the waveform structure. Transmit filter, receiver filter, and density of symbols in time-frequency plane determine the available resource opportunities jointly for the other-user interference mitigation by using POT, as exemplified in Fig. 2. Besides, further utilization of the waveform structure via non-orthogonal schemes along with POT lead to a trade-off for uncoordinated networks: *other-user interference versus self-interference*. This trade-off is desirable in an uncoordinated network as long as self-interference is handled via self-interference cancellation methods, e.g., equalization. In the following subsections, orthogonality of schemes is stressed in conjunction with POT. POT with orthogonal schemes and non-orthogonal schemes are investigated theoretically along with numerical results and their potential drawbacks.

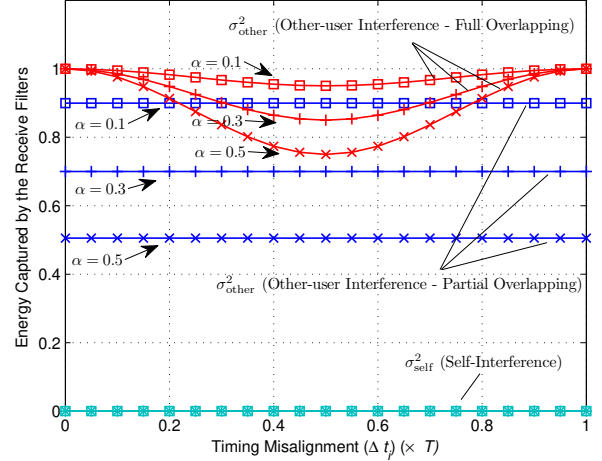
A. Partially Overlapping Tones with Orthogonal Schemes

For orthogonal schemes, transmitter and receiver utilize the same prototype filter, i.e., $g_{mk}^\epsilon(t) = \gamma_{mk}^\epsilon(t)$. In addition, inner products of the different basis functions derived from the prototype filter yield zero correlations, i.e., $\langle g_{nl}^\epsilon(t), \gamma_{mk}^\epsilon(t) \rangle = \delta_{nlmk}$. Many fundamental schemes, e.g., OFDM, FMT, and FBMC, rely on orthogonality. In digital communication, orthogonality in a multicarrier scheme is generally perceived as a necessary condition. It simplifies the receiver algorithms significantly and provides optimum signal-to-noise ratio (SNR) performance in AWGN channels. Besides these features, orthogonal schemes have another fundamental property due to orthogonal basis functions at the receiver: the energy of a signal before the projection onto receive filters is equal to the energy after the projection onto receiver filters. This is typically expressed through the Plancherel formula¹ given by

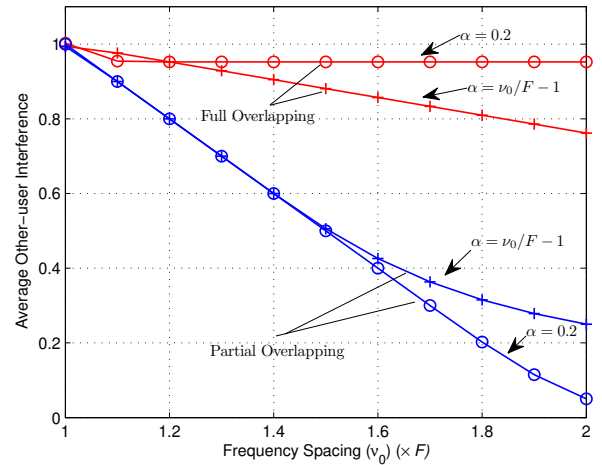
$$\|s(t)\|^2 = \sum_{m,k} |\langle s(t), u_{mk}(t) \rangle|^2, \quad (15)$$

where $s(t)$ is an arbitrary signal, and $\{u_{mk}(t)\}$ is a set of orthogonal basis functions. Assume that $s(t)$ is the interfering signal. When an orthogonal transformation, e.g., discrete Fourier transformation (DFT), is applied to $s(t)$ at the receiver, the total amount of the interference does not change after the transformation. This issue leads to an undesirable result: only way to *mitigate* the other-user interference is to discard some of subcarriers or to construct an *incomplete* Gabor system, i.e., $\tau_0\nu_0 > 1$ [2], [3], which causes less spectrally efficient schemes. In other words, POT with orthogonal schemes would be beneficial only when some of subcarriers are not utilized

¹It corresponds to Parseval's theorem for Fourier series.



(a) Impact of timing misalignment when root raised cosine filter is employed along with FMT.



(b) Trade-off between spectral efficiency and other-user interference.

Fig. 3. Other-user interference mitigation without introducing self-interference, but loss in spectral efficiency.

or $\tau_0\nu_0 > 1$. Indeed, norm-preserving feature of orthogonal transformations at the receivers explain *why orthogonal schemes do not directly provide immunity against the other-user interference*.

POT offers intentional CFO between the different links based on the fact that timing synchronization between TPs in an uncoordinated network is a challenging issue. However, the intentional CFO approach also introduces some constraints on the waveform structure. For example, orthogonal multicarrier schemes which provide non-overlapping subcarriers in frequency domain, e.g., FMT, complies with the intentional CFO approach introduced by POT. However, POT might not be as beneficial as in the case of FMT to the schemes where the orthogonality is maintained strictly on certain localizations in the time-frequency plane, as in OFDM. Considering this issue, analyses throughout the study are performed based on FMT.

In Fig. 3, considering timing misalignment between one aggressor and the victim, Δt_i is swept for one symbol period when $\Delta f_i = \nu_0/2$. FMT is generated based on root-raised-

cosine (RRC) filter. Note that RRC filter is a band-limited filter and the excess bandwidth of the RRC filter is controlled via a roll-off factor of α , where $0 \leq \alpha \leq 1$. In Fig. 3(a), $\sigma_i^2(\Delta t_i, \Delta f_i)$ is calculated numerically, based on (13). In case of full overlapping, $\sigma_i^2(\Delta t_i, \Delta f_i)$ is mitigated maximally when $\Delta t_i = 0.5 \times T$, $\tau_0 = T$, and $\nu_0 = (1 + \alpha) \times F$. This is because of the reduction of the ICI components maximally due to the additional guard bands, when timing misalignment occurs. In case of partial overlapping, impact of Δt_i is removed totally, and $\sigma_i^2(\Delta t_i, \Delta f_i)$ is significantly reduced since the receive filters reject the main portion of the interference, depending on the utilized α . Assuming the aggressor interference has a uniform timing misalignment characteristics, trade-off between spectral efficiency and other-user interference is given for two different FMT cases in Fig. 3(b). When ν_0 is set to $(1 + \alpha) \times F$, $\sigma_i^2(\Delta t_i, \Delta f_i)$ decreases for both full overlapping and partial overlapping due to the less ICI components with the timing misalignment, as given in Fig. 3(a). When α is fixed to 0.2, other-user interference is mitigated more via partial overlapping, since this approach provides more gap in frequency for other-user interference mitigation.

Major concern of using POT with orthogonal schemes might be having less spectral efficient transmission for the sake of other-user interference mitigation. However, as indicated before, it allows the devices interrupted by the interference to achieve a better BER performance with a simple approach.

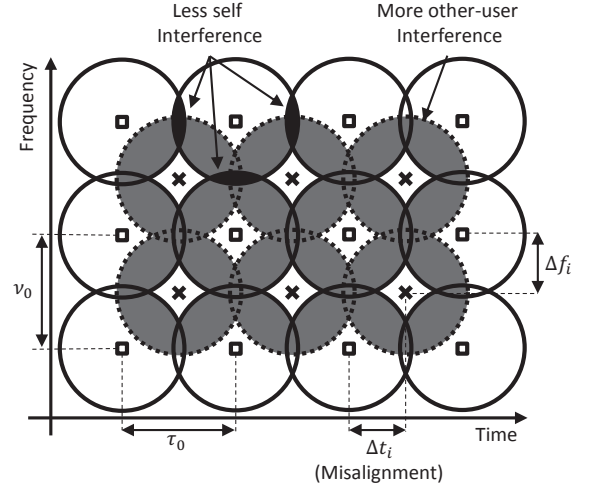
B. Partially Overlapping Tones with Non-orthogonal Schemes

Similar to the orthogonal schemes, transmitter and receiver utilize the same prototype filters for non-orthogonal structures, i.e., $g_{mk}^e(t) = \gamma_{mk}^e(t)$. However, inner products of the different basis functions do not yield zero correlations, i.e., $\langle g_{nl}^e(t), \gamma_{mk}^e(t) \rangle \neq \delta_{nlmk}$. For example, non-orthogonal frequency division multiplexing (NOFDM) can be constructed by using the rectangular lattice of OFDM with non-Nyquist transmit filters and receive filters, e.g., Gaussian functions. For non-orthogonal schemes, the utilized basis functions at the receiver also corresponds to a nonorthogonal transformations, i.e., $\langle \gamma_{nl}^e(t), \gamma_{mk}^e(t) \rangle \neq \delta_{nlmk}$. In that case, the condition given in (15) is relaxed as

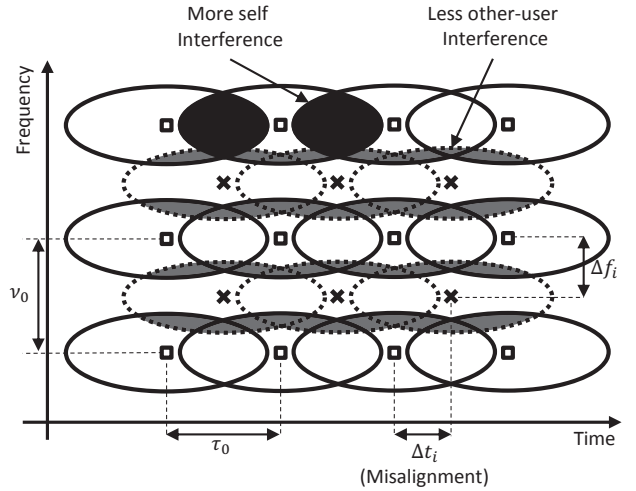
$$A \|s(t)\|^2 \leq \sum_{m,k} |(s(t), u_{mk}(t))|^2 \leq B \|s(t)\|^2, \quad (16)$$

where $\{u_{mk}(t)\}$ is a set of non-orthogonal elements, A and B are the lower bound and upper bound, respectively, and $0 < A \leq B < \infty$. Based on (16), when a non-orthogonal transformation is applied at the receiver, the energy of $s(t)$ does not have to be preserved after the transformation. In other words, the non-orthogonal transformations at the receivers are able to alter the amount of the observed interference energy. Hence, when POT is taken into account with non-orthogonal schemes, it is possible to mitigate other-user interference even when $\tau_0 \nu_0 = 1$.

In order to understand the utilization of POT with non-orthogonal schemes, assume that $\tau_0 \nu_0 = 1$ and the transmit pulse shape and the receive filter are Gaussian filters. Gaussian



(a) Less self-interference, but more other-user-interference.



(b) More self-interference, but less other-user-interference.

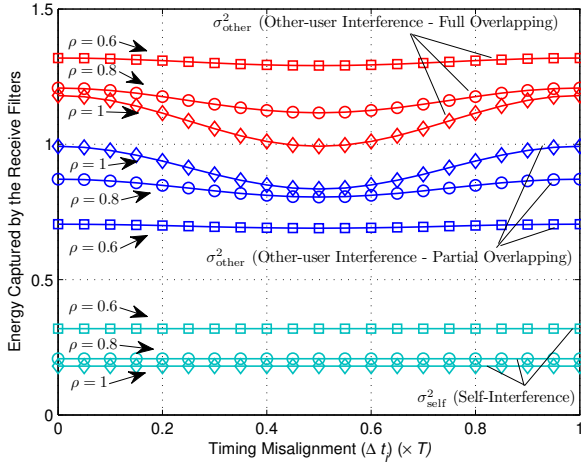
Fig. 4. Illustration for the trade-off between self-interference and other-user interference with the concept of POT. The desired signal and interfering signal are represented as solid and dashed lines, respectively.

filter is the optimally-concentrated pulse in time-frequency domain and it is expressed as

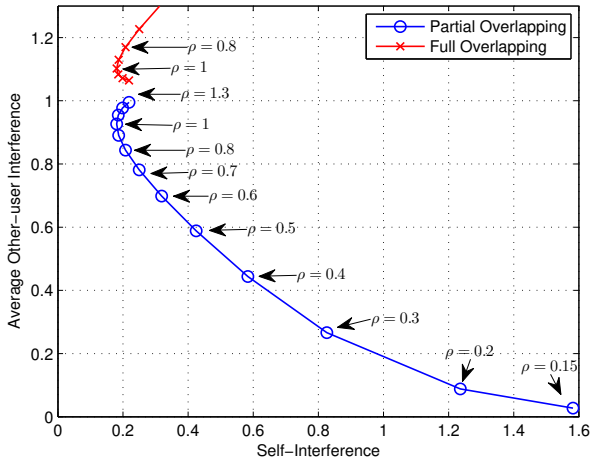
$$p(t) = (2\rho)^{1/4} e^{-\pi\rho t^2}, \quad (17)$$

where ρ is the control parameters for the dispersion of the pulse in time and frequency and $\rho > 0$. While the selection of $\rho = 1$ yields a Gaussian filter that has isotropic dispersion in time and frequency, smaller ρ causes more dispersion in time domain and less dispersion in frequency domain. Since Gaussian filter is not a Nyquist filter, consecutive symbols overlap more with smaller ρ , yielding more self-interference in time, i.e., ISI. However, introducing more ISI is also beneficial to mitigate the other-user interference, when POT is considered, as illustrated in Fig. 4(a) and Fig. 4(b) for $\Delta f_i = \nu_0/2$. In other words, non-orthogonal schemes yield a trade-off between the other-user interference and self-interference by exploiting the POT.

Considering the density of the symbols on time-frequency plane of the victim RP, it is important to emphasize the differences between faster-than-Nyquist (FTN) signaling [34]



(a) Impact of timing misalignment when Gaussian filter is employed.



(b) Trade-off between self-interference and other-user interference.

Fig. 5. Other-user interference mitigation without loss in spectral efficiency and power, but at the expense of self-interference.

and POT with non-orthogonal schemes. In FTN signaling, the density of the symbols in time-frequency plane is increased more than Nyquist rate, i.e., $\tau_0 \nu_0 < 1$, intentionally. However, each individual link operates at the Nyquist rate, i.e., $\tau_0 \nu_0 = 1$, for POT. The time-frequency plane of the victim RP is packed due to the aggressors' signals, which is common in co-channel interference problems. In addition, POT does not suggest a structured symbol packing into the time-frequency plane, as in FTN signaling. It allows timing misalignment among the individual links.

Similar to the investigations given in Section IV-A, Δf_i is set to $\nu_0/2$ and Δt_i is swept for one symbol period. Impact of timing misalignment is given in Fig. 5(a). In case of full overlapping, when $\Delta t_i = 0$, the receive filter has full correlation with the concentric symbol of the aggressor and partial correlations with the neighboring symbols. Hence, the total energy after the correlation becomes more than 1. In case of partial overlapping, receive filters only capture energy from only the neighboring symbols of aggressors,

which yields that $\sigma_{\text{self}}^2 < 1$ as in Fig. 5(a). In Fig. 5(b), the trade-off between self-interference and average other-user interference is given, assuming uniform timing misalignment. As in Fig. 5(b), Gaussian filter provides flexible trade-off between self-interference and other-user interference.

There are two potential drawbacks of this approach: 1) necessity for a self-interference cancellation method, e.g., equalization, since the filters do not satisfy Nyquist criterion and 2) colored noise due to the non-orthogonal receiver filters. For the first issue, the introduced complexity due to self-interference cancellation method might be preferable in comparison with the complexities of the methods for handling *asynchronous* other-user interference. For the second point, note that non-orthogonal transformations always introduce correlation between samples [3]. If a sequence-based equalizer, e.g., maximum likelihood sequence estimator (MLSE), is employed, a whitening filter should also be utilized to improve the performance of the receiver. Note that assuming the small link distances for the pairs, noise might become a secondary problem when interference is a dominant issue.

V. AVERAGE BER ANALYSIS

In this section, average BER analysis is provided for POT for orthogonal schemes that do not introduce self-interference as discussed in Section IV-A. To obtain theoretical (but tractable) BER analysis, a useful method for BER calculations introduced in [35] is combined with spatial PPP approaches [20], [21], [24]. First, BER is expressed along SINR given in (11). Then, its expected value is obtained considering other-user interference. Its computation complexity is significantly reduced by using spatial PPP and ambiguity function. For the trade-off introduced in Section IV-B, investigation on BER performance is performed through the numerical analysis in Section VI, since achievable BER performance depends highly on the employed self-interference cancellation method at the receiver.

Closed-form expression for BER of a square M -QAM in AWGN channel is readily available in the literature and it is given by

$$\text{BER}(SNR) = \sum_q^{\sqrt{M}-2} c_q \text{erfc} \left((2q+1) \sqrt{\frac{SNR}{2}} \right) \quad (18)$$

where M is the constellation size, c_q are the constants depending on the modulation order and $\sum_{q=0}^{\sqrt{M}-2} c_q = 1/2$ [36]. For instance, $c_q = \{1/2\}$ and $q = \{0\}$ for 4-QAM and $c_q = \{3/8, 2/8, -1/8\}$ and $q = \{0, 1, 2\}$ for 16-QAM, respectively.

By substituting (11) into (18), BER is obtained for given I_{total} , G_ϵ , and d_ϵ as

$$\begin{aligned} \text{BER}(E_b/N_0 | G_\epsilon, I_{\text{total}}, d_\epsilon) \\ = \sum_{q=0}^{\sqrt{M}-2} c_q \text{erfc} \left(\frac{2q-1}{\sqrt{2}} \sqrt{\frac{G_\epsilon}{I_{\text{total}} + \frac{M-1}{3 \log_2 M} \frac{1}{E_b/N_0}}} \right). \end{aligned} \quad (19)$$

Since the target is to calculate average BER under interference, the terms, I_{total} , and G_ϵ , have to be averaged out. In order to obtain average BER, we refer to following lemma introduced in [35]:

Lemma-1: Let x and y be unit-mean exponential and arbitrary non-negative random variables, respectively. Then

$$\mathbb{E}_{x,y} \left[\operatorname{erfc} \left(\sqrt{\frac{x}{ay+b}} \right) \right] = 1 - \frac{1}{\sqrt{\pi}} \int_0^\infty \frac{e^{-z(1+b)}}{\sqrt{z}} \mathcal{L}_y(az) dz$$

where $\mathcal{L}_y(z) = \mathbb{E}_y[e^{-yz}]$ is the moment generation function (MGF) with negative argument (or Laplace transformation) of random variable y .

If Lemma-1 is applied to (19) (see e.g., [17], [18], [35], [37]), average BER is obtained as

$$\begin{aligned} \text{BER}(E_b/N_0, d_\epsilon) &= \sum_{q=0}^{\sqrt{M}-2} c_q \left(1 - \frac{1}{\sqrt{\pi}} \int_0^\infty \frac{e^{-z(1+\frac{2}{(2q+1)^2} \frac{M-1}{3 \log_2 M} \frac{1}{E_b/N_0})}}{\sqrt{z}} \right. \\ &\quad \left. \times \mathcal{L}_{I_{\text{total}}} \left(\frac{2z}{(2q-1)^2} \right) dz \right), \quad (20) \\ &= \frac{1}{2} - \frac{1}{\sqrt{\pi}} \sum_{q=0}^{\sqrt{M}-2} c_q \int_0^\infty \frac{e^{-z(1+\frac{2}{(2q+1)^2} \frac{M-1}{3 \log_2 M} \frac{1}{E_b/N_0})}}{\sqrt{z}} \\ &\quad \times \mathcal{L}_{I_{\text{total}}} \left(\frac{2z}{(2q+1)^2} \right) dz. \quad (21) \end{aligned}$$

Therefore, the complexity introduced by (19) reduces to calculate Laplace transformation of I_{total} . In the following subsections, Laplace transformation of I_{total} is calculated in cases of single aggressor and multiple aggressors.

A. Single Aggressor

If only i th aggressor is considered, the Laplace transformation of the total interference is obtained as

$$\begin{aligned} \mathcal{L}_{I_{\text{total}}}(z) &= \mathbb{E}_{I_{\text{total}}} [e^{-zI_{\text{total}}}] \\ &\stackrel{(a)}{=} \mathbb{E}_{I_{\text{self}}} [e^{-zI_{\text{self}}}] \times \mathbb{E}_{I_i} [e^{-zI_i}] = \mathbb{E}_{I_i} [e^{-zI_i}] \\ &\stackrel{(b)}{=} \int_0^{T_0} \frac{f_{\Delta t_i}(\Delta t_i)}{1 + z d_\epsilon \frac{b-\beta b}{10} d_i^{\frac{\beta b}{10}} r_i^{\frac{-b}{10}} \sigma_i^2(\Delta t_i, \Delta f_i)} d\Delta t_i \quad (22) \end{aligned}$$

where (a) follows from the independent assumption of random variables I_i and I_{self} and the assumptions of zero self-interference via orthogonal schemes, (b) is because of the exponential distribution of I_{other} and the randomness of timing misalignment. Considering the uniform timing misalignment assumption and being a constant function of $\sigma_i^2(\Delta t_i, \Delta f_i)$ respect to Δt_i , as in Fig. 3(a), (22) is simplified as

$$\mathcal{L}_{I_{\text{total}}}(z) = \frac{1}{1 + z d_\epsilon \frac{b-\beta b}{10} d_i^{\frac{\beta b}{10}} r_i^{\frac{-b}{10}} \sigma_i^2(\Delta f_i)} \quad (23)$$

B. Multiple Aggressors

When multiple aggressors exist in the network, the choice of Δf_i within the link affects the performance of POT. In order to avoid the coordination, it is assumed that Δf_i is selected randomly from the set Ω given by $[\psi_0, \psi_1, \dots, \psi_r, \dots]$. The selection is performed based on a probability mass function (PMF) where p_r corresponds to the probability of r th intentional CFO. Based on this assumption, the Laplace transformation of the total interference is obtained as

$$\begin{aligned} \mathcal{L}_{I_{\text{total}}}(z) &= \mathbb{E}_{I_{\text{total}}} [e^{-zI_{\text{total}}}] \\ &\stackrel{(a)}{=} \mathbb{E}_{I_{\text{self}}} [e^{-zI_{\text{self}}}] \times \mathbb{E}_{\Phi, I_i} [e^{-z\sum_{i \in \Phi} I_i}] \\ &\stackrel{(b)}{=} \mathbb{E}_{\Phi, I_i} [e^{-z\sum_{i \in \Phi} I_i}] = \mathbb{E}_{\Phi} \left[\prod_{i \in \Phi} \mathbb{E}_{I_i} [e^{-zI_i}] \right] \quad (24) \\ &\stackrel{(c)}{=} \exp \left[-2\pi\lambda \int_{r_{\min}}^\infty (1 - \mathbb{E}_{I_i} [e^{-zI_i}]) \nu d\nu \right] \quad (25) \end{aligned}$$

where (a) follows from the independent assumption of random variables I_{other} and I_{self} , (b) is because of zero self-interference via orthogonal schemes, and (c) is caused by the probability generating functional of PPP, which states $\mathbb{E}_{\Phi} [\prod_{i \in \Phi} f(x)] = \exp \int_{\mathbb{R}^2} (1 - f(x)) dx$ for an arbitrary function $f(x)$ and the assumption of i.i.d. interference from each aggressor I_i and independent Φ from other random variables in the interference function I_{other} [21]. Considering randomness of aggressors' distances d_i , $\mathbb{E}_{I_i} [e^{-zI_i}]$ is obtained as

$$\begin{aligned} \mathbb{E}_{I_i} [e^{-zI_i}] &= \mathbb{E}_{d_i, G_i} [e^{-z \frac{P_i}{P_\epsilon} G_i}] \\ &= \sum_r p_r \int_0^\infty \frac{f_u(u)}{1 + z d_\epsilon \frac{b-\beta b}{10} u^{\frac{\beta b}{10}} \nu^{\frac{-b}{10}} \sigma_i^2(\psi_r)} du \quad (26) \end{aligned}$$

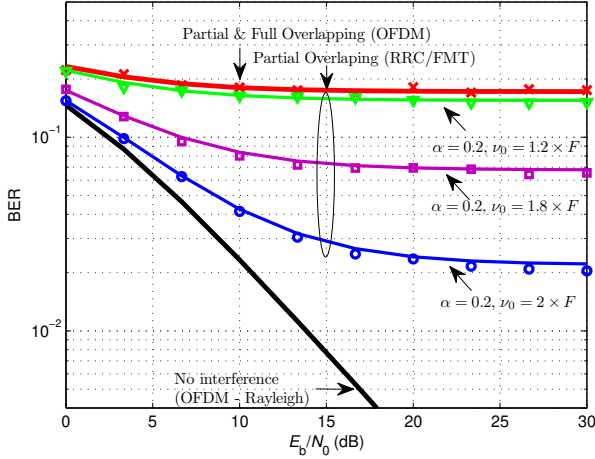
which is based on the Laplace transformation of an exponentially disturbed random variable, uniform timing misalignment assumption, and being a constant function of $\sigma_i^2(\Delta t_i, \Delta f_i)$ respect to Δt_i . In (26), the probability density function (PDF) of d_i is given by $f_u(u) = 2\pi\lambda u e^{-\lambda\pi u^2}$ [22]. Then, $\mathcal{L}_{I_{\text{total}}}(z)$ is obtained as

$$\begin{aligned} \mathcal{L}_{I_{\text{total}}}(z) &= \exp \left[-2\pi\lambda \int_{r_{\min}}^\infty \right. \\ &\quad \left. \left(1 - \sum_r p_r \int_0^\infty \frac{2\pi\lambda u e^{-\lambda\pi u^2}}{1 + z d_\epsilon \frac{b-\beta b}{10} u^{\frac{\beta b}{10}} \nu^{\frac{-b}{10}} \sigma_i^2(\psi_r)} du \right) \nu d\nu \right] \quad (27) \end{aligned}$$

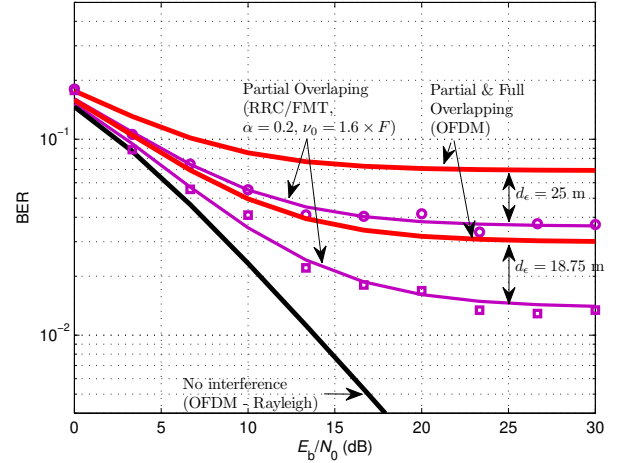
by substituting (26) into (25). Note that (27) does not always yield a closed-form solution since $\int_0^\infty \frac{x e^{-ax^2}}{1+bx^c} dx$ produces an expression in terms of standard mathematical functions depending on a, b , and c . Nonetheless, (27) does not require Monte Carlo simulations.

VI. NUMERICAL RESULTS

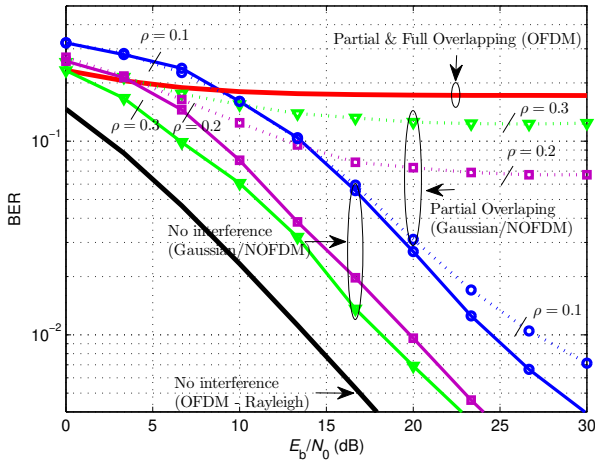
Numerical results are given in order to validate analytical findings with simulations and to investigate the performance of uncoordinated networks along with POT. In the simulations,



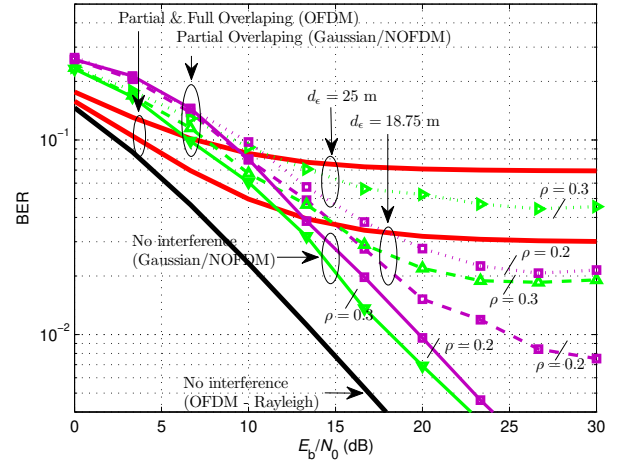
(a) RRC/FMT/4QAM (Solid lines: Analytical results based on (21) and (23)).



(a) RRC/FMT/4QAM (Solid lines: Analytical results based on (21) and (27)).



(b) Gaussian/NOFDM/4QAM.



(b) Gaussian/NOFDM/4QAM.

Fig. 6. BER performance with partial overlapping when there is a single aggressor.

Fig. 7. BER performance with partial overlapping when there are multiple aggressors modeled with PPP.

POT with orthogonal schemes and POT with non-orthogonal schemes are exhibited by utilizing FMT with RRC filter and zero forcing equalization and by using NOFDM with Gaussian filter and symbol-spaced MLSE equalization, respectively. For MLSE, 7 taps are utilized for each subcarrier and trace-back depth for MLSE is set to 20. Unless otherwise stated, numerical result are obtained for Rayleigh channels.

In Fig. 6, impact of partial overlapping is presented in Rayleigh channel for the aforementioned trade-offs when a dominant aggressor interrupts the transmission with the equal received signal power (i.e., signal-to-interference ratio (SIR) is set to 0 dB). In Fig. 6(a), α is set to 0.2 and the subcarrier spacing is swept from $1.2 \times F$ to $2 \times F$, referring to the POT with orthogonal schemes. Also, simulation results are verified with the theoretical results based on (21) and (23). As it can be seen in Fig. 6(a), efficacy of POT in the BER performance increases with the subcarrier spacing, which also causes less spectrally efficient schemes. In Fig. 6(b), the same analysis is performed for NOFDM to address the POT with non-orthogonal schemes. When other-user interference

do not exist, orthogonal schemes reach the Rayleigh bound and introduce superior BER performance compared to non-orthogonal schemes. This is mainly because of the fact that MLSE loses its optimality under the colored noise caused by the non-orthogonal transformation at the receiver. However, when the other-user interference exists, orthogonal schemes capture the total amount of the other-user interference and BER performance deteriorates significantly. In contrast to orthogonal waveforms, non-orthogonal schemes become notable with the concept of POT under the other-user interference. By providing sufficient non-orthogonality, e.g., $\rho = 0.1$, BER performance remains the same of the case without other-user interference for NOFDM for low to medium SNR, as it can be seen in Fig. 6(b). Essentially, the results show that BER performance is enhanced without sacrificing the spectral efficiency at the expense of complexity at the receiver.

In Fig. 7, impact of POT on BER performance is shown when there are multiple aggressors. In the simulation, the path

loss is modeled with the parameters given in [38] as

$$L(d) = 11.8 + 45 \log_{10}(f_c) + 40 \log_{10}(d/1000) \quad (28)$$

where f_c is the carrier frequency in MHz (3500 MHz) and d is the distance in meters. Using given parameters, the path loss formula is calculated as $L(\cdot) = 51.3 + 40 \log(\cdot)$ where the argument is in terms of meters. Accordingly, a and b are set to 51.3 and 40, respectively. The intensity of TP and r_{\min} are set to $1/(\pi 50^2)$ and 25 m, respectively. In order to see the best possible BER performance, all aggressors' signals are partially overlapped with the desired signal. Then, BER curves are obtained for different victim link distance d_e . As expected, BER is directly related to the user distance. Especially, the degradation becomes severe for the users located at far distances. In Fig. 7(a), it is shown that orthogonal schemes allow better BER performance with the concept of POT by losing their spectral efficiencies. Also, simulation results match with the theoretical results based on (21) and (27). In Fig. 7(b), the impact of non-orthogonal schemes on BER performance are shown for the same scenario and better BER performance is obtained for high E_b/N_0 without any spectral efficiency loss, but complexity at the receiver. Considering Fig. 6(b) and Fig. 7(b), it is important to emphasize that one may obtain the optimum ρ , considering the amount of the attainable self-interference and the amount of mitigated other-user interference. Although the selection of $\rho = 0.1$ significantly improve the BER performance when the amount of the other-user interference is equal to signal power, the same scheme might not yield optimum BER performance when other-user interference becomes weaker due to the path loss. Essentially, this issue indicates that there is a point where non-orthogonality starts to be harmful. Therefore, the best selection of ρ depends on the equalizer performance and the amount of the other-user interference.

VII. CONCLUDING REMARKS

In this study, by allowing intentional CFO between the interfering links, other-user interference is mitigated in an uncoordinated network without any timing constraints via orthogonal or non-orthogonal schemes. For a well-coordinated network, transmission over orthogonal schemes might lead to better performance compared to non-orthogonal schemes due to the absence of self-interference. However, when other-user interference is inevitable and significant in an uncoordinated network, spectral efficiency has to be sacrificed for orthogonal schemes in order to allow other-user interference mitigation. Specifically, schemes which allow non-overlapping subcarriers in frequency, e.g., FMT, complies with the intentional CFO approach to avoid timing misalignment problems with POT. As opposed to orthogonal waveforms, non-orthogonal schemes come into the prominence along with POT for an interesting reason; self-interference problem is easier than other-user interference problem in an uncoordinated networks. By utilizing non-orthogonal waveforms, POT is able to change the type of interference from other-user interference to self-interference. This is beneficial when the receiver has proper self-interference cancellation mechanisms. Especially, it is

promising when two pairs sharing the same spectrum are close to each other.

Throughout the study, POT is presented for two intentional CFO levels, i.e., f_c and $f_c + \nu_0/2$. Although the POT with two intentional CFO levels heuristically matches to two-users scenarios, it might be a suboptimum solution for the multiple-user scenarios. However, it is possible to utilize multiple CFO levels to extend POT to multiple-user scenarios. In addition, when the difference between the power levels of interfering signal and desired signal are significantly large, well-known interference cancellation methods, e.g. successive interference cancellation (SIC), might provide better results than POT. However, the combination of POT and interference cancellation techniques can increase the performance substantially. Since POT is able to increase the difference between the norm of interference and the norm of desired signal power, POT is also able to increase the separability of the signals.

ACKNOWLEDGMENT

This study has been supported by InterDigital Communications Inc.

REFERENCES

- [1] C. Shannon, "Communication in the presence of noise," *Proceedings of the IEEE*, vol. 86, no. 2, pp. 447–457, 1998.
- [2] A. Sahin, I. Güvenc, and H. Arslan, "A survey on multicarrier communications: prototype filters, lattice structures, and implementation aspects," *CoRR*, vol. abs/1212.3374v2, 2012.
- [3] W. Kozek and A. Molisch, "Nonorthogonal pulses shapes for multicarrier communications in doubly dispersive channels," *IEEE J. Select. Areas Commun. (JSAC)*, vol. 16, no. 8, pp. 1579–1589, Oct. 1998.
- [4] D. Lopez-Perez, I. Guvenc, G. De la Roche, M. Kountouris, T. Quek, and J. Zhang, "Enhanced intercell interference coordination challenges in heterogeneous networks," *IEEE Wireless Communications*, vol. 18, no. 3, pp. 22–30, 2011.
- [5] J. Andrews, "Interference cancellation for cellular systems: a contemporary overview," *IEEE Wireless Communications*, vol. 12, no. 2, pp. 19–29, 2005.
- [6] S. Verdu, *Multuser Detection*. Cambridge University Press, 1998.
- [7] V. Cadambe and S. Jafar, "Interference alignment and degrees of freedom of the k -user interference channel," *IEEE Trans. Information Theory*, vol. 54, no. 8, pp. 3425–3441, 2008.
- [8] A. Mishra, V. Shrivastava, S. Banerjee, and W. Arbaugh, "Partially overlapped channels not considered harmful," *SIGMETRICS Perform. Eval. Rev.*, vol. 34, no. 1, pp. 63–74, Jun. 2006.
- [9] Y. Ding, Y. Huang, G. Zeng, and L. Xiao, "Channel assignment with partially overlapping channels in wireless mesh networks," in *Proceedings of the 4th Annual International Conference on Wireless Internet*, ser. WICON '08, ICST, Brussels, Belgium, 2008, pp. 38:1–38:9.
- [10] Y. Cui, W. Li, and X. Cheng, "Partially overlapping channel assignment based on node orthogonality for 802.11 wireless networks," in *Proc. IEEE International Conference on Computer Communications (INFOCOM)*, 2011, pp. 361–365.
- [11] O. Ileri, I. Hokelek, H. Arslan, and E. Ustunel, "Improving data capacity in cellular networks through utilizing partially overlapping channels," in *Proc. IEEE Conference on Signal Processing and Communications Applications (SIU)*, Apr. 2011, pp. 1121–1124.
- [12] P. Duarte, Z. Fadlullah, A. Vasilakos, and N. Kato, "On the partially overlapping channel assignment on wireless mesh network backbone: A game theoretic approach," *IEEE J. Select. Areas Commun. (JSAC)*, vol. 30, no. 1, pp. 119–127, 2012.
- [13] M. Fu, H. Crussiere and M. Helard, "Spectral efficiency optimization in overlapping channels using TR-MISO systems," in *Proc. IEEE Wireless Communications and Networking Conference (WCNC)*, Apr. 2013.
- [14] V. Chandrasekhar, J. Andrews, and A. Gatherer, "Femtocell networks: a survey," *IEEE Commun. Mag.*, vol. 46, no. 9, pp. 59–67, Sep. 2008.

- [15] M. Sahin, I. Guvenc, and H. Arslan, "Opportunity Detection for OFDMA-Based Cognitive Radio Systems with Timing Misalignment," *IEEE Trans. Wireless Commun.*, vol. 8, no. 10, pp. 5300–5313, Oct. 2009.
- [16] A. Sahin, I. Guvenc, and H. Arslan, "Analysis of uplink inter-carrier-interference observed at femtocell networks," in *Proc. IEEE International Conference on Communications (ICC)*, 2011, pp. 1–6.
- [17] K. Hamdi and Y. Shobowale, "Interference analysis in downlink OFDM considering imperfect intercell synchronization," *IEEE Trans. Veh. Tech.*, vol. 58, no. 7, pp. 3283–3291, Sep. 2009.
- [18] Y. Medjahdi, M. Terre, D. L. Ruyet, D. Roviras, and A. Dziri, "Performance analysis in the downlink of asynchronous OFDM/FBMC based multi-cellular networks," *IEEE Trans. Wireless Commun.*, vol. 10, no. 8, pp. 2630–2639, Aug. 2011.
- [19] A. Sahin, E. Guvenkaya, and H. Arslan, "User distance distribution for overlapping and coexisting cell scenarios," *IEEE Wireless Commun. Lett.*, vol. 1, no. 5, pp. 432–435, Oct. 2012.
- [20] M. Win, P. Pinto, and L. Shepp, "A mathematical theory of network interference and its applications," *Proceedings of the IEEE*, vol. 97, no. 2, pp. 205–230, 2009.
- [21] J. Andrews, F. Baccelli, and R. Ganti, "A tractable approach to coverage and rate in cellular networks," *IEEE Trans. Commun.*, vol. 59, no. 11, pp. 3122–3134, Nov. 2011.
- [22] T. D. Novlan, H. S. Dhillon, and J. G. Andrews, "Analytical modeling of uplink cellular networks," *CoRR*, vol. abs/1203.1304, 2012.
- [23] H. Dhillon, R. Ganti, F. Baccelli, and J. Andrews, "Modeling and analysis of K-tier downlink heterogeneous cellular networks," *IEEE J. Sel. Areas Commun.*, vol. 30, no. 3, pp. 550–560, Apr. 2012.
- [24] P. Pinto and M. Win, "Communication in a Poisson field of interferers—part I: Interference distribution and error probability," *IEEE Trans. Wireless Commun.*, vol. 9, no. 7, pp. 2176–2186, 2010.
- [25] X. Lin, J. G. Andrews, and A. Ghosh, "A comprehensive framework for device-to-device communications in cellular networks," *CoRR*, vol. abs/1305.4219, 2013.
- [26] D. Gabor, "Theory of communication. part 1: The analysis of information," *Journal of the Institution of Electrical Engineers - Part III: Radio and Communication Engineering*, vol. 93, no. 26, pp. 429–441, 1946.
- [27] P. Sondergaard, "Finite discrete Gabor analysis," 2007.
- [28] C. Tellambura and D. Senaratne, "Accurate computation of the MGF of the lognormal distribution and its application to sum of lognormals," *IEEE Trans. Commun.*, vol. 58, no. 5, pp. 1568–1577, May 2010.
- [29] N. Mehta, J. Wu, A. Molisch, and J. Zhang, "Approximating a sum of random variables with a lognormal," *IEEE Trans. Wireless Commun.*, vol. 6, no. 7, pp. 2690–2699, Jul. 2007.
- [30] M. Marey and H. Steendam, "Analysis of the narrowband interference effect on OFDM timing synchronization," *IEEE Trans. Sig. Proc.*, vol. 55, no. 9, pp. 4558–4566, 2007.
- [31] M. Morelli and M. Moretti, "Robust frequency synchronization for OFDM-based cognitive radio systems," *IEEE Trans. Wireless Commun.*, vol. 7, no. 12, pp. 5346–5355, 2008.
- [32] P. Bello, "Characterization of randomly time-variant linear channels," *IEEE Trans. Commun. Syst.*, vol. 11, no. 4, pp. 360–393, Dec. 1963.
- [33] G. Cherubini, E. Eleftheriou, and S. Olcer, "Filtered multitone modulation for very high-speed digital subscriber lines," *IEEE J. Select. Areas Commun.*, vol. 20, no. 5, pp. 1016–1028, June 2002.
- [34] J. Anderson, F. Rusek, and V. Owall, "Faster-Than-Nyquist signaling," *Proceedings of the IEEE*, vol. 101, no. 8, pp. 1817–1830, 2013.
- [35] K. Hamdi, "A useful technique for interference analysis in Nakagami fading," *IEEE Trans. Commun.*, vol. 55, no. 6, pp. 1120–1124, Jun. 2007.
- [36] K. Cho and D. Yoon, "On the general BER expression of one- and two-dimensional amplitude modulations," *IEEE Trans. Commun.*, vol. 50, no. 7, pp. 1074–1080, 2002.
- [37] K. Hamdi, "Precise interference analysis of OFDMA time-asynchronous wireless ad-hoc networks," *IEEE Trans. Wireless Commun.*, vol. 9, no. 1, pp. 134–144, Jan. 2010.
- [38] Report ITU-R M.2135, "Guidelines for evaluation of radio interface technologies for IMA-Advanced."